

Ultra Wide Band BALUN/180° Power Divider Using Microstrip – Slotline –Microstrip Transition

U. L. Rohde^{1,2}, A. K. Poddar^{1,2}, S. Pegwal³, V. Madhavan¹, S. K. Koul³, M. Abegaonkar³, M. A. Silaghi²

¹Synergy Microwave Corporation, Paterson, New Jersey, USA

²University of Oradea, Faculty of Electrical Engineering and IT, Romania

³Centre for Applied Research in Electronics, IIT-Delhi, New Delhi, India

Abstract— A novel UWB (ultra wideband) BALUN/180° Power Divider utilizing the broadband characteristics of microstrip – slotline transition is reported. The measured operational frequency range of the BALUN on RO4003C substrate is 4GHz–45GHz, corresponding to a typical insertion loss of 4±1dB with an amplitude and phase imbalance of under ±1dB and ±7° respectively. Simulation and measurement of the design on LTCC substrates show reduced loss of around 3.5±1dB with amplitude and phase imbalance of under ±1dB and ±4° respectively, in addition to an increased operational frequency range of 8GHz–90GHz, and reduction in the physical dimensions to 3 mm x 8 mm. Simulations and initial measurement with sapphire substrate have shown the capability of the design to hold good up to 130 GHz.

Keywords—Ultra wideband (UWB); BALUN; Microstrip; Slotlines; Low temperature co-fired ceramic (LTCC)

I. INTRODUCTION

A Balun is a critical microwave device or circuit which converts an unbalanced signal to a balanced one. Antennas, push pull amplifiers, frequency multipliers, frequency mixers are just a subset of a wide variety of circuits utilizing the Balun in their design. Balun being a building block for these devices implies that the performance of the Balun needs to be within appropriate limits for the proper functioning of its end product.

Several types of ultra wideband planar balun have been proposed in the past, some utilizing substrate integrated waveguide or tapered sections while others utilizing 180° hybrids or involving microstrip to CPW or CPS transitions. However, most are limited in the frequency range of operation. This work makes use of the ultra broadband nature of microstrip to slotline transitions in conjunction with the orientation of the input and two output microstrip lines with respect to the slotline to create an UWB balun, the evolution and design details of which are provided in the following sections [1]-[2].

II. DESIGN AND EVOLUTION

A. Evolution

Coupling between two microstrip lines placed on the top metallization layer with a slotline placed perpendicular to the two lines on the bottom layer of a single layer PCB was studied. The geometry shown in Fig. 1 is such that the microstrip input line and the slotline lying on the top (red) and bottom (blue) metallization planes cross each other perpendicularly in a way that the cross junction between the two lines is $\lambda_{mg}/4$ and $\lambda_{sg}/4$ away from the open and short end of the microstrip and slotline respectively, where λ_{mg} and λ_{sg} are the guide wavelengths in microstrip and the slotline. All cross junctions are designed in a similar fashion. The results achieved from this study resulted in

extending this design to three microstrip lines with one input (i/p) and two equi-phased and equal power split output (o/p) ports (step 2). On further modification by mirroring one of the output ports around the axis of the slotline as shown in step 3 of Fig. 1, the two outputs were equal power split but 180° out of phase. However, the microstrip open end and slotline short end being narrowband cause the performance of the balun to be limited to only a few tens of GHz. Significant improvement of bandwidth was achieved on replacing the microstrip open and slotline short ends with broadband conical stubs (step 4). The top and bottom view photograph of the fabricated Balun on RO4003c substrate is shown in Fig. 2.

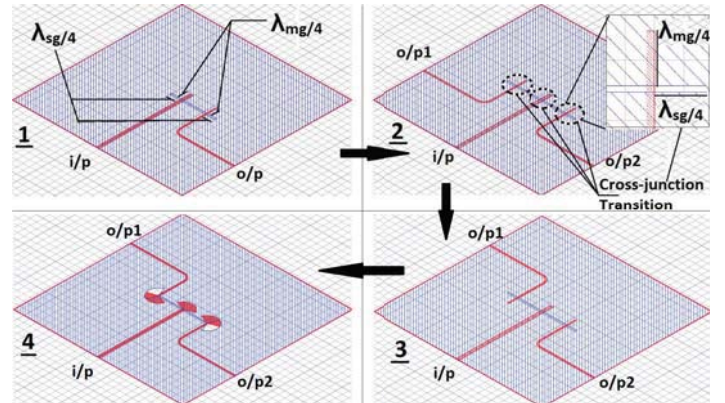


Fig. 1 Evolution of UWB Balun

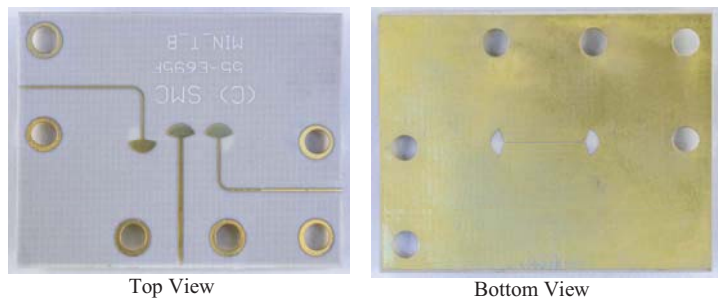


Fig. 2 Fabricated Balun on RO4003c, 8mil substrate height,

B. Equivalent Circuit of Balun Design

Starting from the equivalent circuit for a simple microstrip to slotline transition [3], the equivalent circuit for the entire balun is derived as shown in Fig. 3. Port 1, 2 and 3 are the input port and two output ports respectively. Z_{im} , Z_{om} and Z_{os} are the input microstrip, output microstrip and slotline characteristic impedances, respectively. θ_{im} , θ_{om} , θ_s and $\theta_{L/2}$ are the electrical lengths of the radial stubs of the input microstrip, output microstrip, slotline and the slotline itself, respectively.

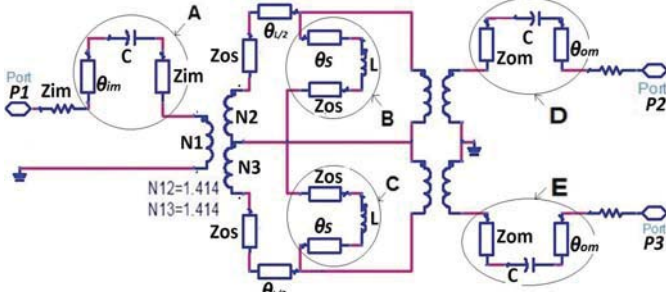


Fig. 3 Equivalent Circuit of Balun

The first transformer on the left represents the input microstrip radial stub to slotline transition and the second pair of transformers represents the slotline radial stub to output microstrip radial stub transitions. The block circled as A is the equivalent circuit associated with the input microstrip radial stub. The blocks B and C are the equivalent circuit associated with the radial stubs on the slotlines. The blocks D and E are associated with the radial stubs of the output microstrip lines.

The equivalent circuit of Fig. 3 needs to be analyzed thoroughly for the right impedance of the slotline in-order to have the optimum return loss for the BALUN. Unlike conventional waveguides, there is no low frequency cut-off which makes it useful in the UWB design, as in a slotline, wave propagating along the slot, has the major electric field component oriented across the slot in the plane of metallization on the dielectric substrate and the mode of propagation is non-TEM in spite of being a two conductor structure and almost transverse in nature.

III. IMPEDANCE ANALYSIS

Impedance analysis of the microstrip and slotline reveal the geometrical parameters needed for an optimum design.

A. Input Impedance

Most microwave sub-systems being matched to 50Ω at the input and output make it imperative for the input microstrip impedance of the Balun to be designed with a width corresponding to 50Ω ; $\sim 0.4\text{mm}$ (16mil) in the proposed design.

B. Slotline impedance

An even and odd mode analysis of the equivalent circuit of Fig. 3 reveals that the input microstrip to slotline structure is similar to a Wilkinson power divider. The analogy between these structures greatly simplifies the preliminary approximation for the optimum characteristic impedance of the slotline which is found to be 70.7Ω . However, this approach does not take into account the parasitics, dispersion effects of the substrate and the effects of slotline-radial to microstrip-radial stub transitions towards the two outputs.

The optimum slotline impedance to achieve a VSWR of one for the ‘slotline–radial stub’ to ‘microstrip–radial stub’ transition at the two output sides is [4]:

$$Z_{os} = \frac{Z_{im}}{n^2} \quad (1)$$

$$\text{where } n = \cos\left(2\pi\frac{d}{\lambda}u\right) - \cot(q_0') \sin\left(2\pi\frac{d}{\lambda}u\right) \quad (2)$$

$$q_0' = 2\pi\frac{d}{\lambda}u + \tan^{-1}\left(\frac{u}{v}\right) \quad (3)$$

$$u = \left[\epsilon_r - \left(\frac{\lambda_0}{\lambda'}\right)^2\right]^{\frac{1}{2}} \quad (4); \quad v = \left[\left(\frac{\lambda_0}{\lambda'}\right)^2 - 1\right]^{\frac{1}{2}} \quad (5)$$

ϵ_r , d , λ_0 and λ' being the permittivity, substrate height, free space wavelength and the guide wavelength respectively. With this analysis, the optimum impedance for a near perfect slotline to microstrip transition through the centers of their radial stubs is found to be 80Ω .

The empirical equations governing the characteristic impedance of a slotline as a function of its physical dimensions for low permittivity materials ($2.22 \leq \epsilon_r \leq 3.8$) is [5].

$$Z_{os} = 60 + 3.69 \sin\left[\frac{(\epsilon_r - 2.22)\pi}{2.36}\right] + 133.5 \ln(10\epsilon_r) \sqrt{\frac{W}{\lambda_0}} + \dots \\ \dots 2.81[1 + 0.011\epsilon_r(4.48 + \ln\epsilon_r)]\left(\frac{W}{d}\right) \ln\left(\frac{100d}{\lambda_0}\right) \\ + 131.1(1.028 - \ln\epsilon_r) \sqrt{\frac{d}{\lambda_0}} \dots \\ + \frac{12.48(1 + 0.18\ln\epsilon_r)W}{d\sqrt{\epsilon_r - 2.06 + 0.85\left(\frac{W}{d}\right)^2}}; \quad \text{for } 0.0015 \leq \frac{W}{\lambda_0} \leq 0.075 \quad (6)$$

$$Z_{os} = 133 + 10.34(\epsilon_r - 1.8)^2 + 2.87[2.96 + (\epsilon_r - 1.582)^2] \dots \\ \dots \sqrt{\left\{\frac{W}{d} + 2.32\epsilon_r - 0.56\right\}\left\{(32.5 - 6.67\epsilon_r)\left(\frac{100d}{\lambda_0}\right)^2 - 1\right\}} \dots \\ - \left(684.45\frac{d}{\lambda_0}\right)(\epsilon_r + 1.35)^2 + 13.23\left[(\epsilon_r - 1.722)\frac{W}{\lambda_0}\right]^2; \\ \text{for } 0.075 \leq \frac{W}{\lambda_0} \leq 1 \quad (7)$$

‘W’ being the width of the slot. The plot of Fig. 4 obtained from the above equations for the proposed Balun design using Rogers - RO4003c substrate with $\epsilon_r = 3.55$, $d = 0.2\text{mm}$, provide the characteristic impedance of the slotline as a function of its physical dimension (W).

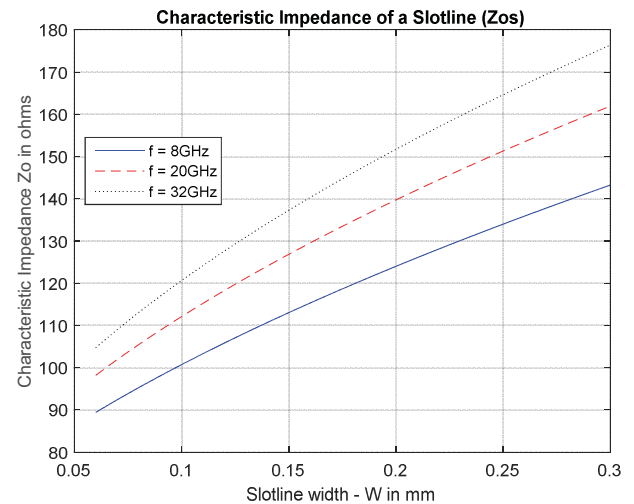


Fig. 4 Characteristic Impedance of a slotline

Finally, a characteristic impedance of $Z_{os} = 100\Omega$ was selected as a compromise between the narrow slot width required to obtain the ideal $Z_{os} = 70.7\Omega$ derived from the even-odd mode analysis for the slotline and the limitations of the available fabrication technique.

C. Output Impedance

The output lines in the form of microstrip make it significantly flexible for use in most microwave and millimeter wave subsystems utilizing Baluns. The characteristic impedance of the output lines are designed to be 75Ω as a trade-off between reduction of mismatch from the 100Ω slotline and the difficulty to fabricate microstrip lines with widths equivalent to impedances greater than 75Ω . These 75Ω lines may be matched to other impedances like 50Ω if the succeeding subsystems require such a matching.

IV. SIMULATION AND MEASUREMENT

After having simulated using HFSS (ver. 14) the fabricated Balun of Fig. 2, the Balun was measured using a ZVA-67, 67GHz Rohde & Schwarz VNA the results of which are shown in the following section.

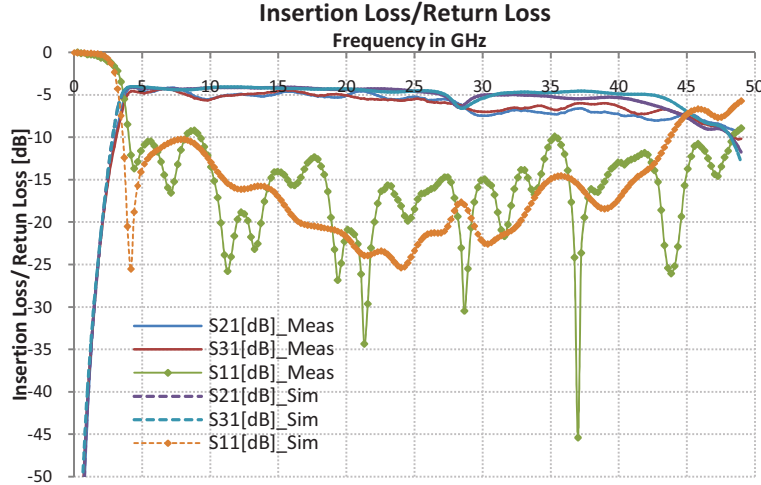


Fig. 5 Insertion/Return Loss of proposed Balun on RO4003c

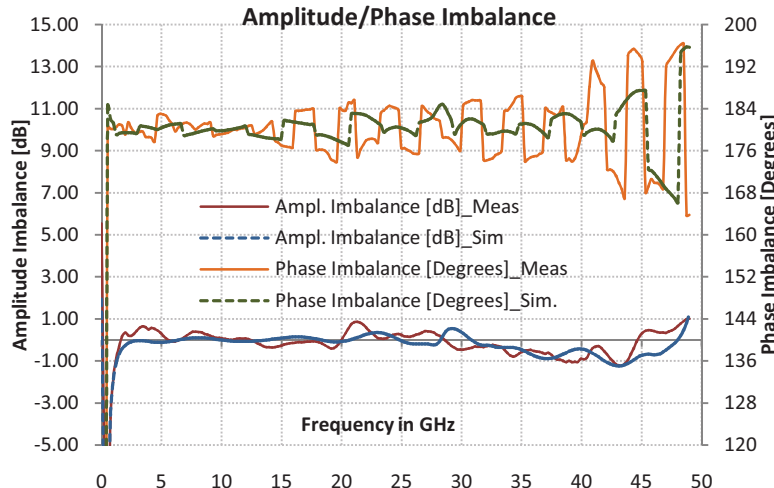


Fig. 6 Amplitude/Phase Imbalance on RO4003c

A. Simulation and Measurement on RO4003c

A Rogers RO4003c dielectric material ($\epsilon_r = 3.55$) of 0.2mm (~8mil) dielectric substrate thickness with 0.5oz of copper was used for fabrication. The simulation and measurements are shown in Fig. 5 as well as Fig. 6.

A close match between the simulation and measured results is obtained. Insertion Loss of each output path of the Balun within a typical of 4 ± 1 dB, with return loss better than 10dB and amplitude and phase imbalance less than ± 1 dB and $\pm 7^\circ$ respectively, over the 4-45GHz band is achieved on a RO4003c substrate board.

The phase jumps seen in Fig. 6 for the simulated and measured phase imbalance can be attributed to the geometrical asymmetry between output radial stubs with respect to the input microstrip line and radial stub. With increasing frequency, the reducing guide wavelengths become comparable to the dimensions of the slotline leading to these phase jumps becoming more severe.

B. Simulation and Measurements on LTCC

Results of the simulation and measurements on RO4003c substrate, motivated in performing simulations of the same design on LTCC using HQW66 ($\epsilon_r = 6.6$) substrate material with 50 um dielectric thickness which has a relatively low dielectric loss ($\tan\delta = 0.0018$) and is suitable for use at millimeter waves. The dimensions of the board are 3 mm x 8 mm. The input and output ports have been designed and optimized for measurements on a probe station with Picoprobe 150 um GSG probes as shown in the HFSS screenshot in Fig. 7.

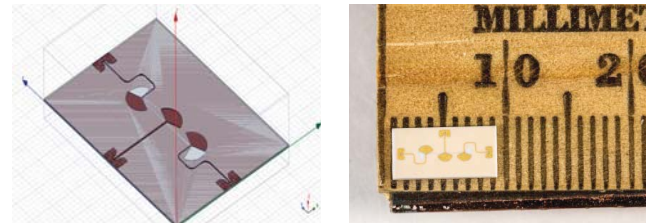


Fig. 7 Balun on LTCC (Copyright: Synergy Microwave Corp., NJ

The design was then fabricated on LTCC substrate as shown in the photograph of the Balun on a millimeter scale ruler. The simulation and measured results of the LTCC Balun are shown in Fig. 8.

Measurements were made on R&S ZVA-110, 110GHz analyzer. The simulations show that the Balun fabricated on LTCC can be comfortably used from 8-90GHz; however, the measured results closely match the simulated results only upto 50GHz in Fig. 8.

Phase jumps similar to Fig. 6 (RO4003c substrate) are observed in Fig. 8 (LTCC substrate) but are found to be much less severe in comparison to Fig. 6 particularly due to the reduced dimensions of the board. Although, included in Table I, these results on LTCC are under further investigation due to the increased mismatch between simulated and measured insertion loss results at frequencies beyond 50GHz.

Similar simulations with sapphire substrate have shown promising results up to 130GHz.

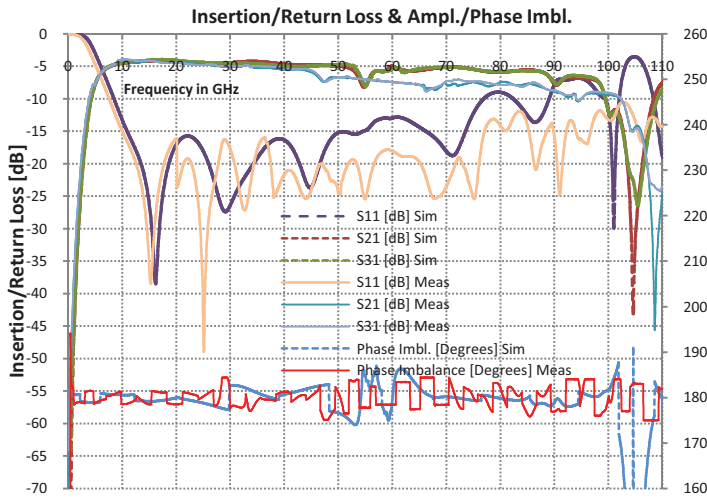


Fig. 8 Insertion Loss and imbalance parameters of Balun on LTCC

C. Comparison Chart

TABLE I. PLANAR BALUN COMPARISON

Balun	Balun Comparison Table		
	Frequency Range	Amplitude/Phase Imbalance	Insertion/Return Loss
[6]	2 – 20 GHz	$\pm 1.2\text{dB}/\pm 9^0$	-
[7]	19 – 29 GHz	$\pm 1\text{dB}/\pm 5^0$	5dB
[8]	2 – 18 GHz	-	1dB
[9]	1.9 – 19 GHz	$\pm 1.4\text{dB}/\pm 5^0$	-
[10]	0.95 - 2.15 GHz	$\pm 1\text{dB}/\pm 10^0$	4dB
This work on RO4003c	4 – 45 GHz	$\pm 1\text{dB}/\pm 7^0$	4dB
This work on LTCC	8-90 GHz	$\pm 1\text{dB}/\pm 7^0$	4dB

V. CONCLUSION

This work presents a novel ultra broadband Balun/180° power divider utilizing the microstrip-slotline-microstrip transition. Measurements of this design fabricated on RO4003c have shown less than $\pm 1\text{dB}$ of amplitude imbalance and $\pm 7^0$ of phase imbalance along with a typical $4\pm 1\text{dB}$ of insertion loss and better than 10dB of return loss over the entire 4-45GHz frequency band. Unlike MMIC Baluns, this planar Balun does not require any tight coupling and the designs of this Balun on LTCC are comparable to the dimensions of MMICs while also providing ultra wide bandwidths. Future research on this Balun

is to be based on negative index metamaterial structures. With the development of MMIC fabrication techniques, metamaterial geared structures are a promising alternative to extended high frequency Balun solutions [11]-[13]. The initial simulation result confirms the increase in the operational frequency to the sub-terahertz regime up to 300 GHz.

ACKNOWLEDGMENT

The authors are thankful to Hirai S. K. Corp., Japan for the manufacturing of designs on LTCC. The authors are also thankful to Synergy Microwave Corp., NJ, USA; Bayerische Akademie der Wissenschaften, Munich, Germany; Fraunhofer EMFT, Munich Germany; Rohde & Schwarz, Munich Germany; CARE Lab IIT Delhi, India; and Drexel University, PA, USA for assistance and help in measurement of fabricated designs.

REFERENCES

- [1] S.B. Cohn, "Slot lines on a dielectric substrate", *IEEE Trans. on MTT*, 172, Feb. 1972.
- [2] K.C. Gupta, R. Garg and I.J.Bahl, "Microstrip Lines and Slot lines", *Artech House*, Norwood, MA, 253, 1979.
- [3] M. M. Zinieris, R. Sloan and L. E. Davis, "A Broadband Microstrip – To – Slotline Transition", *Microwave and Optical Technology Letters*, Vol. 18, No. 5, Aug 5 1998.
- [4] J. B. Knorr, "Slotline Transitions," *IEEE Trans. Microwave Theory Tech.*, Vol MTT-22, pp.548-554, 1974.
- [5] R. Janaswamy, D. H. Schaubert, "Characteristic Impedance of a wide slotline on Low-Permittivity Substrates," *IEEE Trans. Microwave Theory Tech.*, Vol MTT-34, No. 8, 1986.
- [6] D. E. Meharry, "Decade bandwidth planar MMIC Balun," *IEEE MTT-S Int. Dig.*, pp.1153-1156, 2006.
- [7] Z. Y. Zhang and K. Wu, "A Broadband Substrate Integrated Waveguide (SIW) Planar Balun," *IEEE Microwave and Wireless component Letters*, vol. 17, no. 12, pp 843-845, Dec 2007.
- [8] L. Sun, B. Du, G. Han, C. Niu, "A New Ultra Wideband Tapered Balun for Improved ELEVEN Antenna," *IEEE 5th Global symposium on Millimeter waves*, pp. 67-69, 2012.
- [9] H. Ta, A. Stameroff, A.V. Pham, "Development of defected ground structure wide bandwidth balun on multilayer organic substrate," *Proc. Asia-Pacific Microw. Conf.*, pp. 1641-1644, Dec 7-10, 2010.
- [10] Y Dai, H Yin, Y Feng, P Li, Q. Han, M. Han, "A LTCC miniaturized Broadband modified Marchand Balun," *IEEE Intl. Symposium on Comm. & Info. Tech.*, 2012.
- [11] A. K. Poddar, "Slow Wave Resonator Based Tunable Multi-Band Multi-Mode Injection-Locked Oscillators" Dr.-Ing.-habil Thesis, BTU Cottbus, Germany, 2014
- [12] S. Kahng, J. Lee, Koon-Tae Kim, and Hyeong-Seok Kim, "Metamaterial CRLH Structure-based Balun for Common-Mode Current Indicator", *Journal of Electr Eng Technol* Vol. 9, No. 1: 301-306, 2014., <http://dx.doi.org/10.5370/JEET.2014.9.1.301>
- [13] N. J. Smith, D. Papantoni, and J. L. Volakis, "Bandwidth Reconfigurable Metamaterial Arrays", *Int. Journal of Antennas and Propagation*, Vol. (2014), Article ID 397576, pp.1-17, <http://dx.doi.org/10.1155/2014/397576>